Experimental analysis of ethanol dual-fuel combustion in a heavy-duty diesel engine: an optimization at low load

Vinícius B. Pedrozo, Ian May, Macklini Dalla Nora, Alasdair Cairns, Hua Zhao

Centre for Advanced Powertrain and Fuels Research, College of Engineering, Design and Physical Sciences, Brunel University London, Uxbridge, London, UB8 3PH, UK

* Corresponding author. *E-mail address*: vinicius.pedrozo@brunel.ac.uk (V. B. Pedrozo).

Highlights

Advanced ethanol-diesel combustion concept using split diesel injections.

Lower NOx and soot emissions than conventional diesel combustion.

Higher indicated efficiency and mitigation of combustion losses at low load operation.

Unmodified heavy-duty diesel engine hardware design.

Abstract

The reduction in engine-out emissions and the demand for alternative energy sources have become essential to achieving sustainability while complying with current and future emissions regulations. Fossil fuels, as gasoline and diesel, are being progressively replaced by renewable sources. In this framework, experimental studies of ethanol dual-fuel combustion in a heavy-duty diesel engine operating at 1200 rpm and 25% load were carried out with the goal to reduce NOx and soot emissions while mitigating combustion losses, considered a significant limiter at low loads. Fuel delivery was in the form of port fuel injection of ethanol and common rail direct injection of diesel. The effect of three ethanol energy fractions of 32, 53, and 68% were explored as well as the impact of several diesel injection strategies on combustion, emissions, and efficiency. Optimization tests were performed for the 53% ethanol energy fraction. The impact of exhaust gas recirculation, intake air pressure, diesel injection split ratio, injection timing, and rail pressure were investigated. The advanced combustion concept of a premixed charge of ethanol ignited by diesel injections reduced NOx levels by 65% and soot emissions by approximately 30% when compared to conventional diesel operation. The split diesel injection strategy also maintained control over the combustion phasing while resulting in increased net indicated efficiency and high combustion efficiency.

Keywords

Dual-fuel combustion; ethanol; split diesel injections; engine-out emissions; combustion losses; low load.

1 Introduction

Heavy-duty (HD) diesel engines have been widely utilized in on and off-road transportation sectors due to their high torque capability, reliability, as well as superior fuel conversion efficiency [1]. However, conventional diesel combustion produces harmful exhaust emissions and can adversely affect the air quality if not controlled by in-cylinder measures and exhaust aftertreatment systems. Engine-out emissions are significantly reduced by aftertreatment technologies, but it typically leads to higher production costs and fuel economy penalties [2]. Alternatively, systems capable of precise control of fuel injection, exhaust gas recirculation (EGR), and intake air temperature can be used to achieve low NOx and particulate matter (PM) emissions, while maintaining or improving thermal efficiency [3,4]. Even so, according to economic growth projections, it is predicted an increase in the demand for petroleum and other energy sources by more than 30% from 2010 to 2040, particularly in Asia, Africa, and America [5]. This may result in elevated prices for liquid fuels and compromise their cost competitiveness, opening opportunities for improved sustainability and greenhouse gas (GHG) emissions reduction via biofuels, such as biodiesel, alcohols, and biogas [6].

Several new combustion concepts aiming to reduce pollutant emissions and fuel consumption while meeting strict emissions and fuel economy (CO_2) regulations have been developed. The most popular combustion technologies are generally centred on improved fuel atomization and mixture preparation, lower local equivalence ratios, reduced peak in-cylinder temperatures, and faster burn rates. This is usually referred to Low Temperature Combustion (LTC) [2]. Among the combustion strategies proposed is Homogeneous Charge Compression Ignition (HCCI). This is characterized by early fuel injections promoting a fully pre-mixed charge, long ignition delays, and short combustion durations. However, the lack of direct control of ignition timing and combustion phasing, particularly under transient conditions, is still the major drawback. It also exhibits elevated combustion losses, combustion noise, and sensitivity to temperature [7–9]. In comparison, some slightly more heterogeneous combustion concepts have been developed. Premixed Charge Compression Ignition (PCCI) [10–13], Partially Premixed Charge Compression Ignition (PPCI) [14], Modulated Kinetics (MK) [15], and Uniform Bulky Combustion System (UNIBUS) [16] name a few. These allow a higher degree of combustion phasing control at low and medium loads while maintaining low soot and NOx emissions. However, these less pre-mixed combustion modes tend to suffer from lower indicated efficiency, increased unburnt hydrocarbons (HC) and carbon monoxide (CO) emissions, and limited load range due to high EGR and boost requirements.

Gasoline Direct Injection Compression Ignition (GDCI) [17,18] and Partially Premixed Combustion (PPC) [19–21] are some alternatives to diesel LTC. They expand the high efficiency window and achieve very low NOx emissions operating up to full load with moderate-high EGR rates. As these concepts utilize gasoline, they do not reduce the dependence on liquid fossil fuels. They also require engine hardware modifications such as the piston and injection system, and ignition or lubricant improvers, depending on the fuel selected. Some drawbacks regarding soot levels at higher loads, due to low air-fuel ratio, accompanied with significant CO and HC emissions at low loads are also reported. Recent PPC studies with renewable fuels, including ethanol, have demonstrated high thermal efficiency and further soot reductions [22–24]. However, high acoustic noise and elevated peak heat release rates have been experienced due to a fast-burn premixed combustion, requiring lower intake air pressures and larger amounts of EGR, which reduce combustion efficiency [25]. The technical challenges of running an engine purely on ethanol make it not a practical solution for HD engines, particularly under cold ambient conditions.

Finally, dual-fuel (DF) combustion, such as Premixed Micro Pilot Combustion (PMPC) [26] and Reactivity Controlled Compression Ignition (RCCI) [27,28], has been developed to overcome the majority of the previously mentioned issues. The concept uses multiple fuels to control the in-cylinder charge reactivity distribution while achieving a wide operating range with near zero levels of NOx and soot, acceptable pressure rise rate (PRR), and very high indicated efficiency [29]. The primary method of fuel delivery is the port fuel injection of a low reactivity fuel (i.e. gasoline, alcohol, propane, natural gas, etc.) to create a well-mixed charge of fuel-air-EGR, while the high reactivity fuel (i.e. diesel) is directly injected into the combustion chamber in small quantities using single or multiple injection strategies [30]. In the case of RCCI combustion, the diesel injections are significantly advanced to promote a more homogeneous mixture. As RCCI is premixed and predominantly controlled by chemical kinetics, its combustion phasing displays sensitivity to variations in the intake air temperature and pressure [30]. Furthermore, the combustion phasing is generally controlled by varying fuel reactivity (i.e. substitution ratio), which might not be the optimum at certain engine loads. Additionally, the majority of RCCI research utilizes gasoline as its primary fuel.

To promote the use of an alternative petroleum product, this paper focused on the utilization of ethanol in a single cylinder HD diesel engine equipped with high pressure common rail diesel injection and port fuel ethanol injection systems. Fundamentally different from RCCI and conventional DF combustion [31,32] injection strategies, the effectiveness of a premixed charge ignited by split diesel injections around firing top dead centre (TDC) was explored. The first diesel injection increased the charge reactivity while the second allowed a more direct control over the combustion phasing.

Early DF results obtained from an optical engine showed that ethanol, an oxygenated biofuel with high knock resistance and high latent heat of vaporization, can suppress soot formation in high temperature regions of the conventional diesel combustion chamber [33]. Recent experimental analyses with ethanol-diesel combustion demonstrated noticeable NOx reductions at engine loads above 0.8 or 1.0 MPa net indicated mean effective pressure (IMEP) [34–38]. However, inferior efficiency accompanied with high CO and unburnt HC emissions (generally around 30 g/kWh at 0.6 MPa IMEP) became a significant limiter at lower loads due to incomplete combustion [39–42].

Considering the previously described background, a systematic study was carried out at 1200 rpm and 25% load (0.615 MPa IMEP) in an attempt to mitigate combustion losses and improve efficiency of ethanol-diesel combustion at low load, while maintaining low levels of NOx and soot emissions.

The effect of three ethanol energy fractions of 32, 53, and 68% were explored as well as the impact of several split diesel injection strategies on combustion, emissions, and efficiency. The aim was to determine the optimum strategy that provides the highest engine efficiency with the lowest emissions, without external EGR. Then, further investigations on the effect of the timing and quantity of the pre-injection were performed over the best ethanol-diesel strategy selected, maintaining a reasonable level of EGR to suppress NOx formation. Finally, the impact of higher intake air pressure and diesel injection pressure were explored. The best DF results were subsequently compared against conventional diesel-only operation.

2 Experimental Setup

The experiments were carried out on a single cylinder HD diesel engine coupled to an eddy current dynamometer. The test cell layout and main engine specifications are depicted in Figure 1 and Table 1, respectively. Measurement device specifications are shown in the Appendix. Two large-volume surge tanks were installed to damp out pressure fluctuations in the intake and exhaust manifolds. Fresh intake air was supplied to the engine by an external compressor system with closed loop control over the pressure. An intake throttle provided fine control over the intake pressure. The fresh air flow rate was measured by a thermal mass flow meter. High-pressure loop cooled external EGR was supplied to the engine by the combination of an EGR valve and an electronically controlled exhaust back pressure valve located downstream the exhaust surge tank.

Auxiliary equipment such as the high-pressure diesel pump (HPP) and the engine coolant and oil pumps are not coupled to the engine but driven by separate electric motors. Coolant and oil temperatures were kept within 353±5 K. Oil pressure was set to 350±10 kPa throughout the experiments. An independent low-pressure system supplied diesel to the common rail injection system. Two Coriolis flow meters were used to measure the diesel flow rate ($\dot{m}_{diesel}$) by considering the total fuel supplied and returned from the injector and the HPP. Ethanol was injected into the intake port through a high flow-rate peak-and-hold port fuel injector (PFI). It was mounted into the intake air manifold so that the spray was directed towards the back of the intake valves, located approximately 0.3 m downstream.

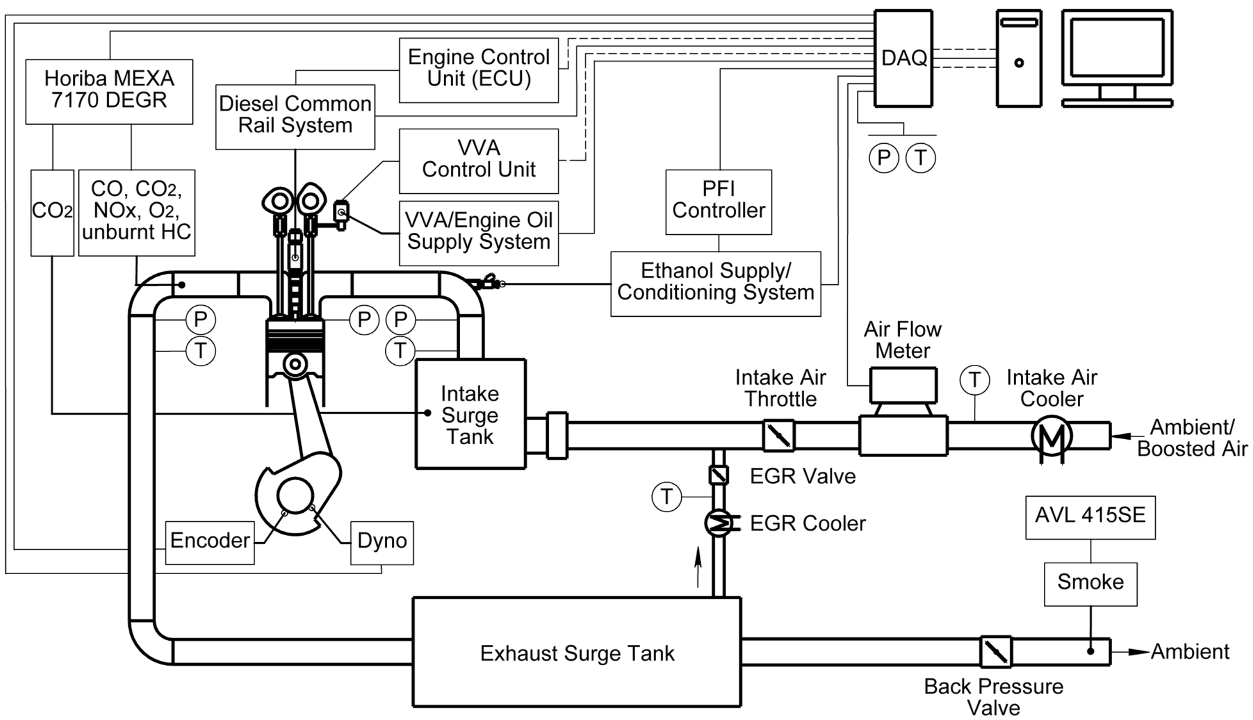

Figure 1 – Schematic diagram of the engine experimental setup.

Table 1 – Single cylinder HD diesel engine specifications.

Parameter	Value
Bore	129 mm
Stroke	155 mm
Swept volume	2026 cm^3
Geometric compression ratio	16.8:1
Maximum in-cylinder pressure	18 MPa
Piston type	Shallow toroidal bowl
Number of valves	4
Diesel injection system	Common rail, inj. pressure of 50 to 220 MPa, centrally mounted diesel injector, 8 holes
Ethanol injection system	PFI peak-and-hold Marelli IWP069, included spray angle of 15°

An in-house injector driver controlled the PFI pulse width, adjusted according to the desired ethanol substitution ratio. The ethanol start of injection (SOI) was set to the firing top dead centre (TDC) to maximize the time for air-fuel mixture preparation before the intake valve opening event. The ethanol mass flow rate ($\dot{m}_{ethanol}$) was obtained from the injector calibration curve. Ethanol injection pressure was continuously monitored by a pressure transducer, so that a constant delta pressure of 300±10 kPa could be maintained across the injector. A heat exchanger held the fuel temperature constant at 293±5 K. The relevant properties of the fuel used in this work are listed in Table 2.

Table 2 – Fuel properties.

Characteristic	Diesel	Ethanol
Product	Gasoil (Ultra Low Sulphur)	Ethyl alcohol
Density at 293 K	827 kg/m^3	789 kg/m^3
Cetane Number	~45	~5
Research Octane Number	~20	~109
Alcohol content	NA	99.1-99.5% (v/v)
Water content	< 0.2 g/kg	< 1.14 (w/w)
Boiling point/range	450-630 K	351 K
Heat of vaporization	~300 kJ/kg	~900 kJ/kg
Carbon content	86.6%	52.1%
Hydrogen content	13.2%	13.1%
Oxygen content	0.2%	34.8%
LHV	42.9 MJ/kg	26.9 MJ/kg

The stoichiometric air/fuel ratio was determined by the conservation of mass of each chemical element in the reactants [43]. The global equivalence ratio was calculated based on the engine-out emissions [44] and confirmed by the air and fuel flow rates. The lower heating value and the indicated specific fuel consumption of the DF combustion mode, LHV_{DF} and $ISFC_{DF}$, respectively, were calculated by the following equations:

$$LHV_{DF} = \frac{\dot{m}_{ethanol} \times LHV_{ethanol} + \dot{m}_{diesel} \times LHV_{diesel}}{(\dot{m}_{ethanol} + \dot{m}_{diesel})} \tag{1}$$

$$ISFC_{DF} = \frac{\dot{m}_{diesel} + \left(\frac{\dot{m}_{ethanol} \times LHV_{ethanol}}{LHV_{diesel}}\right)}{P_i} \times 10^3 \tag{2}$$

where Pi represents the net indicated power.

The in-cylinder pressure was measured by a piezoelectric pressure sensor. Intake and exhaust pressures were measured by two water cooled piezoresistive absolute pressure sensors. The intake valve lift profile was obtained by measuring the displacement of the valve spring retainer with an S-DVRT-24 displacement sensor. Temperatures and pressures at relevant locations were measured by K-type thermocouples and pressure gauges, respectively.

Two National Instruments data acquisition (DAQ) cards were used to acquire the signals from the measurement device. While a high speed DAQ card received the crank angle resolved data synchronized with an optical encoder of 0.25 crank angle degrees (CAD) resolution, a lower speed DAQ card acquired the low frequency engine operation conditions. The data was calculated and displayed live by an in-house developed software, and recorded every one hundred cycles. The IMEP was calculated over the entire cycle. The apparent net heat release rate (HRR), denoted by (dQ_n/dt), was calculated using the following well-known equation:

$$\frac{dQ_n}{dt} = \frac{\gamma}{\gamma-1} p \frac{dV}{dt} + \frac{1}{\gamma-1} V \frac{dp}{dt} \tag{3}$$

where, γ is the ratio of specific heats, t is time, and V and p stand for in-cylinder volume and pressure, respectively. Since the absolute value of heat released is not as important to this study as the bulk shape of the curve with respect to crank angle, a γ of 1.33 was assumed. CA50 is the crank angle of 50% mass fraction burnt (MFB). Ignition delay was defined as the period of time between the diesel start of injection and start of combustion (SOC), set to 0.3% MFB point of the average cycle. Cycle-to-cycle variability was measured by the coefficient of variation of the IMEP (COV_IMEP), defined as the ratio of the standard deviation in IMEP and the mean IMEP over the sampled cycles.

Exhaust emissions were measured by a Horiba MEXA-7170 DEGR emission analyser equipped with a heated line and a high pressure module to allow high-pressure samplings. The EGR rate was calculated by the ratio of intake and exhaust CO_2 concentrations measured by the same analyser. According to [45–47], the determination of the actual hydrocarbons emissions measured by the flame ionization detector (FID) needs to be calibrated for the combustion of oxygenated compounds due to relative insensitivity of the equipment toward alcohols and aldehydes. Therefore, the FID response to ethanol was corrected by the method developed in [46] with an updated factor of 0.68 [47]. This correction uses a second order polynomial and the volumetric ethanol content as an input. Smoke was measured by an AVL 415SE Smoke Meter. The results were converted from FSN to mg/m^3, according to [48]. The calculation of specific exhaust gas emissions was based on [49], with NOx and CO emissions corrected to the wet basis. Finally, combustion efficiency was calculated by:

$$\eta_C = 1 - \frac{\left(ISCO \times LHV_{CO} + ISHC \times LHV_{dual-fuel}\right) \times \frac{P_i}{10^3}}{(\dot{m}_{ethanol} \times LHV_{ethanol} + \dot{m}_{diesel} \times LHV_{diesel})} \quad (4)$$

where *ISCO* and *ISHC* represent the net indicated specific emissions of CO and unburnt HC in g/kWh, respectively.

3 Test Conditions

The test point selected for this study was an engine speed of 1200±5 rpm and a load of 0.615±0.005 MPa IMEP. This point is close to operation points #3 and #8 of the World Harmonized Stationary Cycle (WHSC) and #7 of the former European Stationary Cycle (ESC13) for HD engines. Figure 2 shows where the test point (white circle with black dots pattern) is located over an estimated speed and load map of a HD diesel engine. The WHSC and ESC13 test cycle points are also displayed. The bigger the circle, the higher is the relative weight of the point. The aim was to mitigate combustion losses and improve efficiency while achieving NOx and soot levels close to Euro VI legislation emissions limits (0.40 and 0.01 g/kWh, respectively), utilizing low levels of intake air pressure and EGR.

The engine is equipped with a prototype variable valve actuation system (VVA). Variable intake valve closing timing (IVC) and the resulting effective compression ratio (ECR) can be selected during the engine operation. The intake valve opening and closing timings were maintained at 372±1 CAD and -147±1 CAD after firing top dead centre (ATDC) thought out the tests, providing an ECR of approximately 15.9:1. MPRR and COV_IMEP limits were set to 2 MPa/CAD and 5%, respectively.

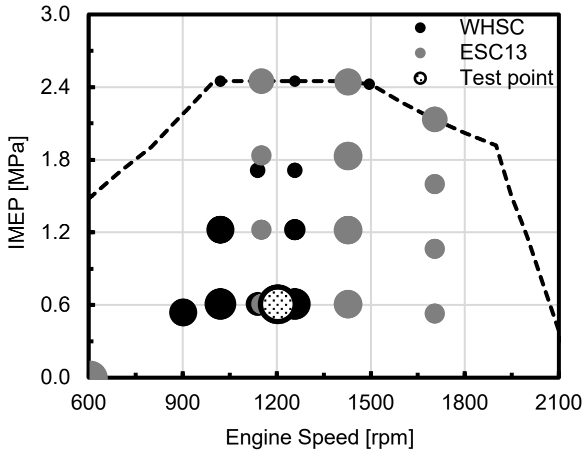

Figure 2 – The selected test point, and the WHSC and ESC13 test cycle points over an estimated HD diesel engine speed- load map.

4 Results and Discussion

4.1 Conventional diesel combustion baseline

The primary objective of these tests was to obtain the best ISFC, NOx and soot trade-off in diesel-only operation by means of moderate amounts of EGR, elevated injection pressures, and optimized SOI. The conventional diesel baseline was performed at four different EGR rates of 0, 10, 21, and 25%. EGR temperature varied from 296 to 354 K as its ratio increased. Intake manifold temperature also rose from 292 K with no EGR to 306 K at 25% EGR. Two intake air pressures of 103 and 125±1 kPa were included as a reference to the DF experiments. A 10 kPa difference between intake air and exhaust gas back pressure was applied throughout the tests to maintain consistent pumping losses. The maximum COV_IMEP observed during these tests was 1.8%.

Rail pressure (RP) was increased from 70 to 125 MPa as larger percentages of EGR were added. A single injection strategy could only be applied in some cases in order to keep the

MPRR under the limit of 2 MPa/CAD. A small pilot injection of approximately 3 mm^3, with a dwell timing of 1 ms (7.2 CAD) and a diesel injection split ratio of 28/72, in average, was used to decrease the pressure rise rates, especially in the cases of higher injection pressures. The split ratio calculation was based on the ratio of the energising time (ET) of each injection to the total energising time. The pilot injection resulted in shorter ignition delay (ID) periods (SOI_2 to SOC), reducing the rate of premixed combustion, represented by the first peak in the heat release diagram (Figure 3). As a result, lower combustion noise (MPRR) was achieved at the expense of higher soot emissions.

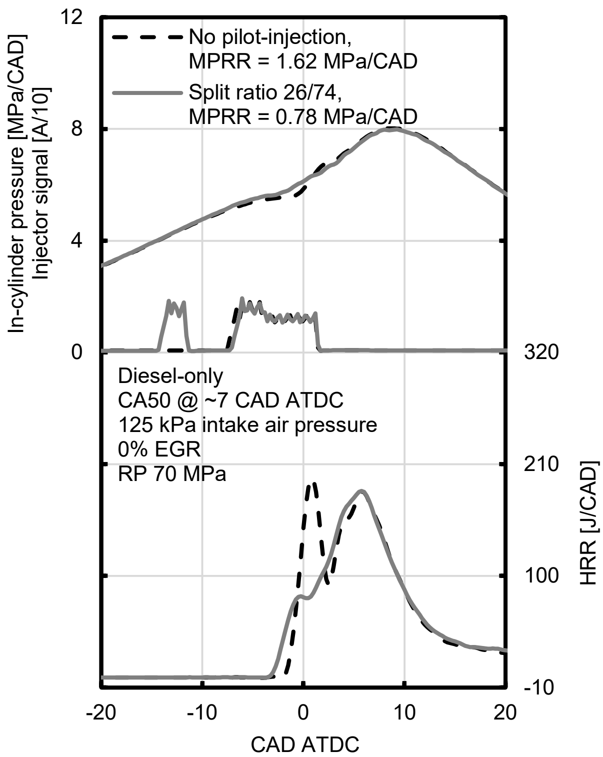

Figure 3 – In-cylinder pressure, injector signal, and HRR curves of conventional diesel combustion running without pilot injection and with a split ratio of 26/74, both at the same intake air pressure and rail pressure.

The sensitivity of the MPRR, ISFC, ISNOx and ISSoot to different intake air and injection pressures, EGR rates, and combustion phasing (CA50) are shown in Figure 4. The legend makes reference to the intake pressure, EGR rate, RP, and diesel injection split ratio. A higher intake air pressure of 125 kPa improved fuel efficiency as leaner mixtures reduced in-cylinder temperatures and subsequent heat transfer losses [50]. Higher oxygen availability and higher injection pressures reduced soot emissions by minimizing fuel-rich combustion and enhancing diesel atomization and mixing. NOx production decreased as more EGR was added due to a lower combustion temperature. This is a result of the higher total heat capacity of the charge and its lower oxygen concentration. These are typical trade-offs of a conventional diesel combustion system and directly related to combustion temperature and local equivalence ratio.

Higher diesel fuel injection pressure and the ‘correct’ EGR level resulted in an optimum NOx/soot trade-off without penalizing fuel consumption. This optimum calibration will be used for future comparisons to the best ethanol-diesel combustion mode. The selected diesel calibration is circled on the curve denoted with “x” markers. It was achieved at an intake air pressure of 125 kPa, a rail pressure of 125 MPa, and 25% EGR, resulting in ISSoot and ISNOx emissions of 0.018 and 2.01 g/kWh, respectively. A detailed summary of the best diesel-only strategy is given in Table 6 and will be discussed later in the paper.

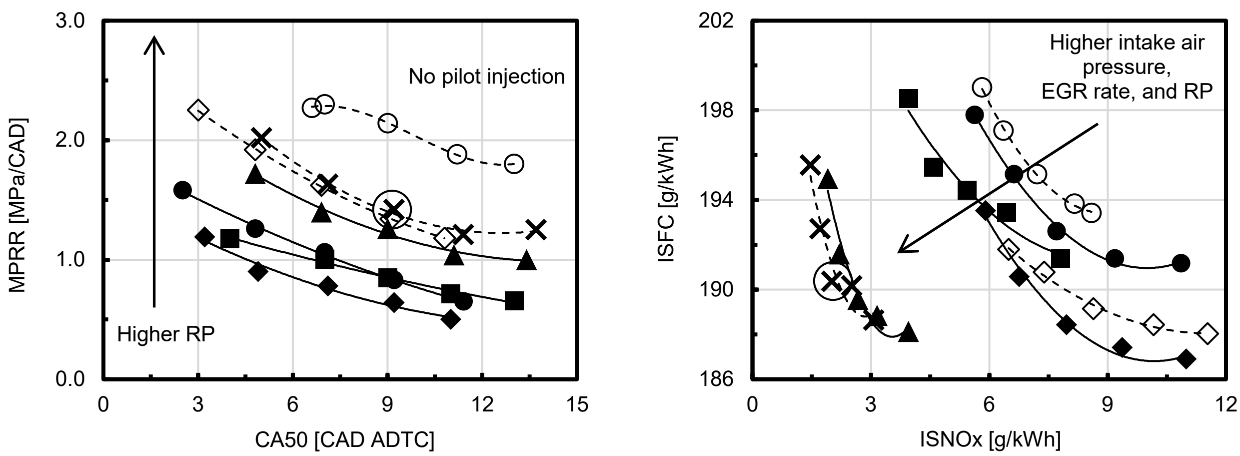

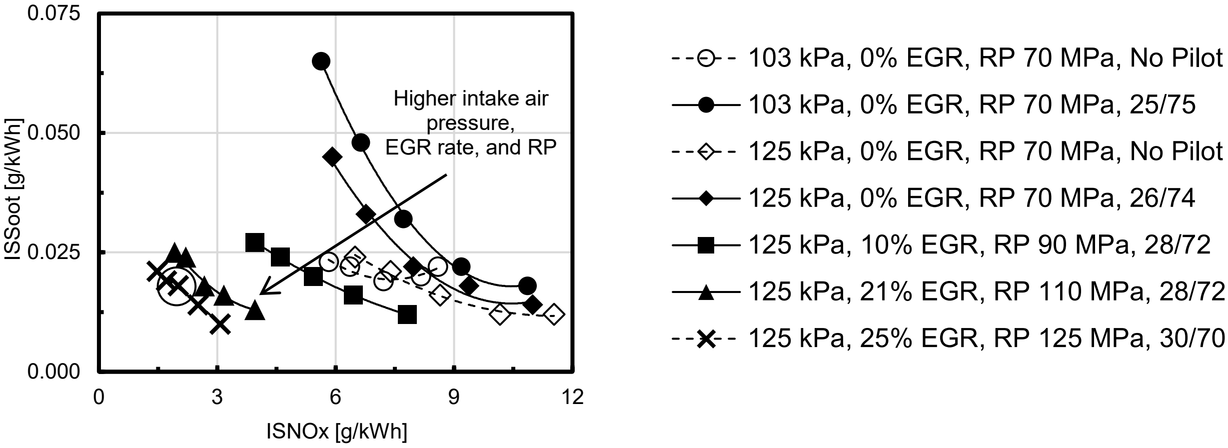

Figure 4 – Conventional diesel combustion sensitivities of MPRR, ISFC, ISNOx and ISSoot to different intake pressures, injection strategies, and CA50.

4.2 Ethanol-diesel operation without EGR

In this section, the optimum ethanol substitution ratio and diesel injection strategy to ignite and efficiently burn the ethanol-air premixed charge is identified. No external EGR was used in this initial phase to reduce the complexity of the test. Intake air and exhaust back pressures were held constant at 103±1 kPa and 113±1 kPa, respectively. Intake air temperature was maintained at 295±3 K throughout this set of experiments. Upon using the conventional diesel baseline injection strategy, ethanol-diesel engine operation had a limited operating range in terms of ethanol substitution ratio and emissions. This was due to a slightly retarded combustion phasing, low combustion efficiency, and diesel knock, as confirmed by prior studies [31,32]. Split diesel injections with different pre and main injection timings and durations were then adopted to increase the range of operation by improving the in-cylinder charge distribution and ignition process.

Three ethanol mass flow rates were tested: 1.24, 1.93, and 2.59 kg/h. These injection quantities were equivalent to substitution ratios of approximately 32, 53, and 68%, denoted by E32, E53, and E68. These ratios are quantified by the ethanol fraction on an energy input basis, defined as the ratio of the energy content of ethanol to the total energy of both fuels. In this test, the start of the second injection (SOI_2) was a result of the stipulated start of the first injection (SOI_1) and the dwell timing (DT) between injections. This differs from RCCI operation, where the first and second injections are delivered at around -60 and -35 CAD ATDC, targeting the squish and the bowl regions of the combustion chamber [51]. The required energising time for the first injection (ET_1) was set using the ECU's application program. The energising time of the second injection (ET_2) was automatically adjusted by the engine speed governor. As the diesel fuel mass injected at each energising time cannot be easily determined and is a function of the temperature of the fuel and the in-cylinder pressure, the estimate of the quantity injected at SOI_1 and SOI_2 was based on the ratio of the energising time of each injection to the total injection time, named split ratio.

Table 3 shows the diesel injection strategies used at each ethanol substitution ratio. The diesel injection pressure was held constant at 70 MPa. A similar test in diesel-only operation was placed beside as a reference for this analysis. The highest pre-injection amount of 0.90 ms could not be tested with E32 because of excessive heat release rate. At E68, an ET_1 of 0.45 ms was not achieved as a short pre-injection close to the second injection did not allow enough time for mixture preparation prior to the start of combustion, causing elevated PRR. An ET_1 of 0.90 ms was removed by the ECU at E68 because ET_2 was too short to be maintained. SOI_2 was kept within -12 to 2 CAD ATDC.

Table 3 – Diesel injection strategies applied at three different ethanol substitution ratios.

	Operating condition			
Parameter	Diesel	E32	E53	E68

Ethanol mass flow rate [kg/h]	0.00	1.24			1.93				2.59	
Diesel inj. split ratio [%]	25/75	28/73	37/63	45/55	31/69	40/60	48/52	60/40	42/58	51/49
ET_1 [ms]	0.45	0.45	0.59	0.75	0.45	0.59	0.75	0.90	0.59	0.75
ET_1 [estimated mm^3]	3	3	10	20	3	10	20	35	10	20
Dwell timing [ms]	1	1	1	3	1	1	3	5	1	3

Figure 5 depicts the ignition delay from SOI_1 and SOI_2 to SOC for those injection strategies showed in Table 3. It is observed that the ignition delay from SOI_1 to SOC steadily rises as the first injection is advanced. Also, DF mode generally exhibited shorter ignition delays than conventional diesel combustion using the same injection strategy. However, the ignition delay increased again as higher ethanol fractions were employed. When the ignition delay between the SOI_2 and the SOC was plotted, negative values were observed for the more advanced and larger pre-injections of diesel, as autoignition of premixed diesel (i.e. ET_1) occurred earlier.

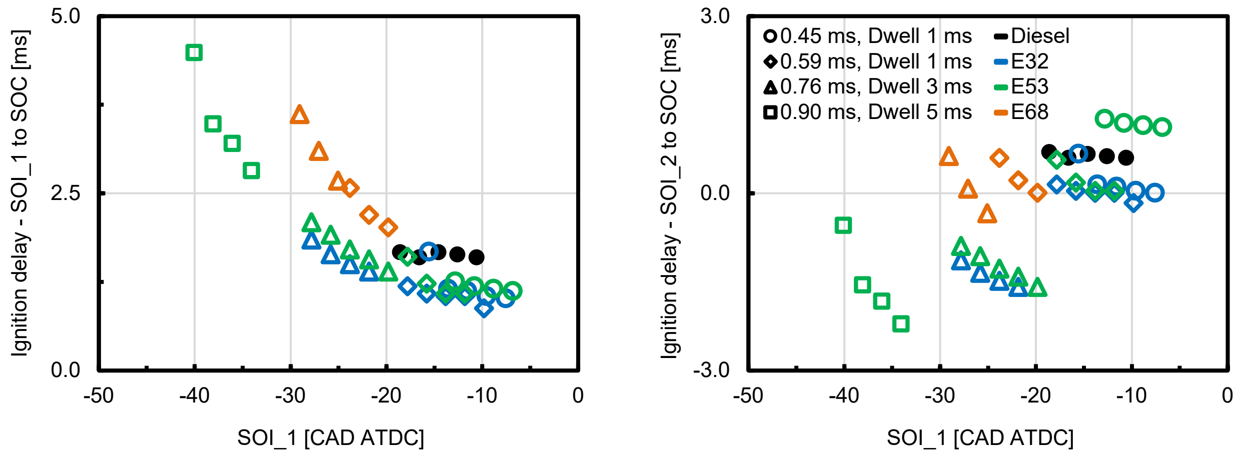

Figure 5 – Ignition delay from SOI_1 and SOI_2 to SOC at different ethanol fractions and diesel injection strategies.

When the SOI_1 was advanced up to -20 CAD ATDC, the combustion phasing was shifted linearly towards TDC, as showed in Figure 6. However, as the SOI_1 was further advanced, no clear correlation between CA50 and SOI_1 could be observed with E53 and E78. The autoignition of the premixed diesel was hindered by the lower reactivity of the ethanol-air charge in the cylinder during the first injection and was more prone to cyclic variations of flow and mixture motion. The combustion duration (CA10-CA90) decreased as the diesel injections were advanced due to the longer mixing period. For the same diesel injection strategy, the combustion duration was also reduced as more ethanol was injected. This is a result of the faster combustion promoted by its homogeneous distribution and flame propagation, generally leading to higher MPRR (Figure 7). Combustion remained stable with COV_IMEP in the range of 1.1 to 2.3% throughout the tests.

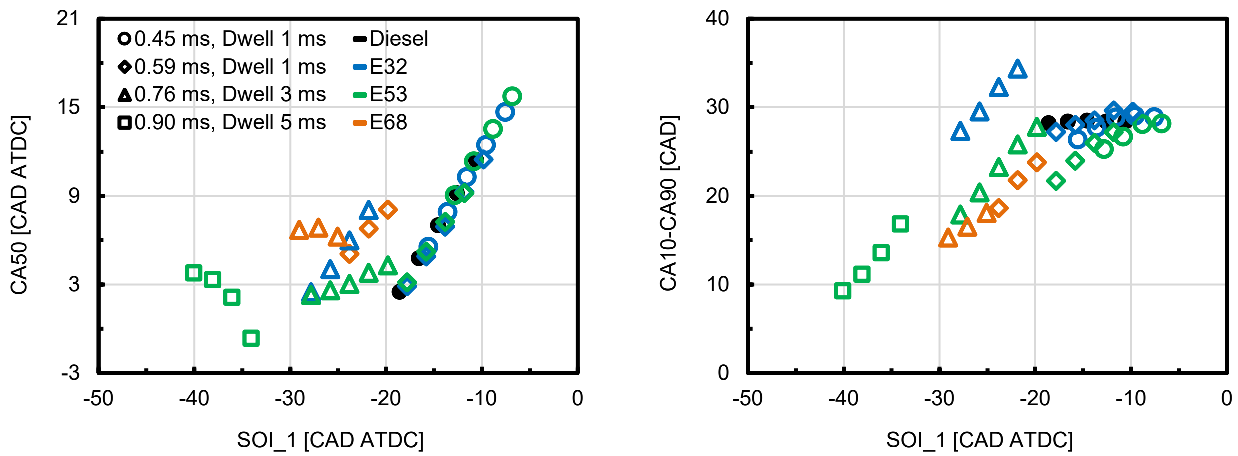

Figure 6 – CA50 and combustion duration at different ethanol fractions and diesel injection strategies.

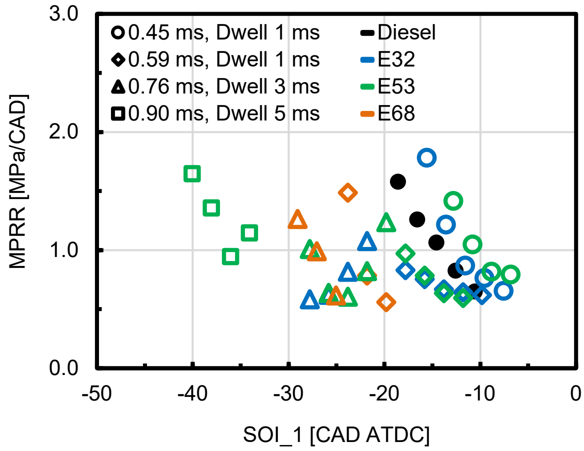

Figure 7 – MPRR at different ethanol substitution ratios and diesel injection strategies.

The emission results in Figure 8 show that a lower NOx/soot emissions trade-off can be achieved using DF combustion when compared to an equivalent diesel operating condition. NOx levels are still high compared to the emissions legislation, but improvements are possible with EGR and will be shown later in the next section. Elevated levels of soot with E32 are a consequence of a shorter ignition delay and high local equivalence ratios. Higher ethanol fractions help with soot reduction, but unburnt HC and CO emissions increase, decreasing combustion efficiency (Figure 9). Low combustion temperature and fuel trapped in the stock diesel piston crevices are the main reasons for this loss [27].

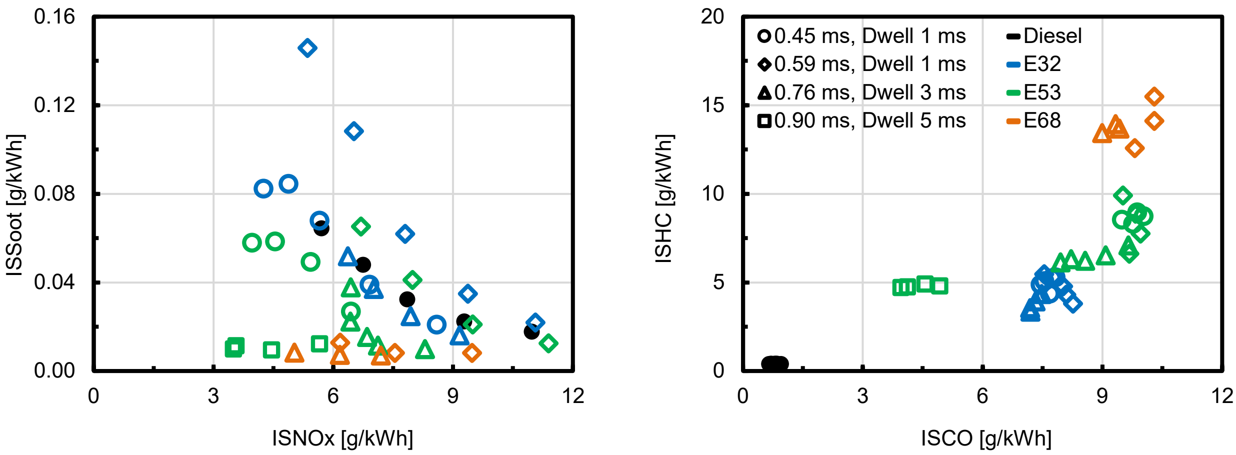

Figure 8 – Indicated emissions at different ethanol substitution ratios and diesel injection strategies.

Based on the results, the optimum calibration strategy was using an ethanol substitution ratio of approximately 53%, with a pre-injection of diesel between -40 to -35 CAD ATDC and a split ratio of ~60/40. Elevated ethanol fractions (i.e. E68) did not completely burn at this specific load, mainly because of excessive in-cylinder temperature reduction. It is believed that higher intake air temperatures could possibly improve combustion efficiency at higher ethanol substitutions [52,53]. Lower substitutions (i.e. E32) did not show advantages, as NOx and soot emissions remained practically unchanged while net indicated efficiency dropped as a result of combustion losses (Figure 9). Table 4 compares the performance and emissions of the best DF operation with those of the conventional diesel combustion running under similar conditions.

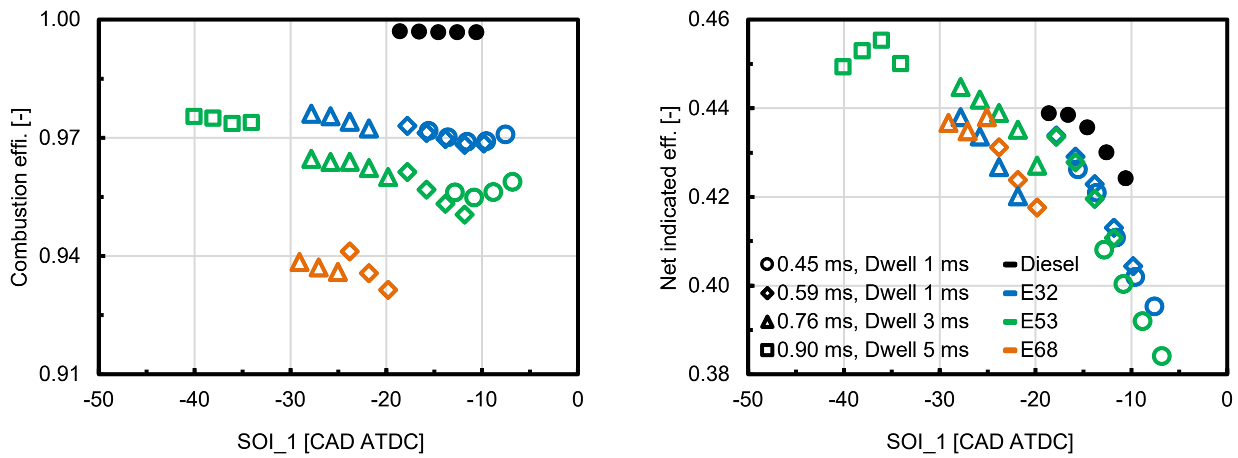

Figure 9 – Combustion and net indicated efficiencies at different ethanol fractions and diesel injection strategies.

Table 4 – Comparison between the best trade-off for ethanol-diesel (E53) and conventional diesel combustion modes running with an intake air pressure of 103 kPa, an RP of 70 MPa, and no EGR.

Parameter	Unit	Diesel	E53
SOI_1	CAD ATDC	-14.5	-36.1

ET_1	ms	0.45	0.90
ET_1	mm^3 (estimated)	3	35
SOI_2	CAD ATDC	-7.3	0.2
Split ratio	%	25/75	60/40
Ignition delay - SOI_2 to SOC	ms	0.67	-1.83
COV_IMEP	%	1.2	1.4
Pmax	MPa	7.12	8.67
MPRR	MPa/CAD	1.07	0.94
CA50	CAD ATDC	7.0	2.1
CA10-CA90	CAD	28.5	13.5
$ISFC_{DF}$	g/kWh	192.6	184.4
Φ_{global}	-	0.48	0.44
ISSoot	g/kWh	0.031	0.011
ISNOx	g/kWh	7.85	3.56
ISCO	g/kWh	0.80	4.56
ISHC	g/kWh	0.42	4.90
Comb. eff.	%	99.7	97.4
Net ind. eff.	%	43.6	45.5

The fuelling and injection strategies used in ethanol-diesel mode resulted in a heat release characteristic of HCCI-type combustion (Figure 10), differing from the typical “double-hump” conventional diesel combustion HRR profile. Low temperature reactions began at around -13 CAD ATDC. However, combustion phasing could still be controlled by the injection timing without the need for large amounts of EGR. Despite the faster and more advanced combustion, the premixed charge promoted lower local peak in-cylinder temperatures and resulted in less than half of the NOx emissions generated by the turbulent diffusion flame of diesel combustion. The well-mixed charge also led to three times less soot, as the formation of fuel-rich zones was minimized.

It can also be observed that the compression work in DF mode was reduced by the ethanol cooling effect [35,54], increasing the net indicated efficiency. The combustion efficiency was slightly lower than conventional diesel combustion. Unburnt HC and CO emissions are of the order of 1200 and 800 ppm, respectively, and are mainly formed by the ethanol fuel trapped in the crevices and squish-volumes of the conventional diesel combustion system.

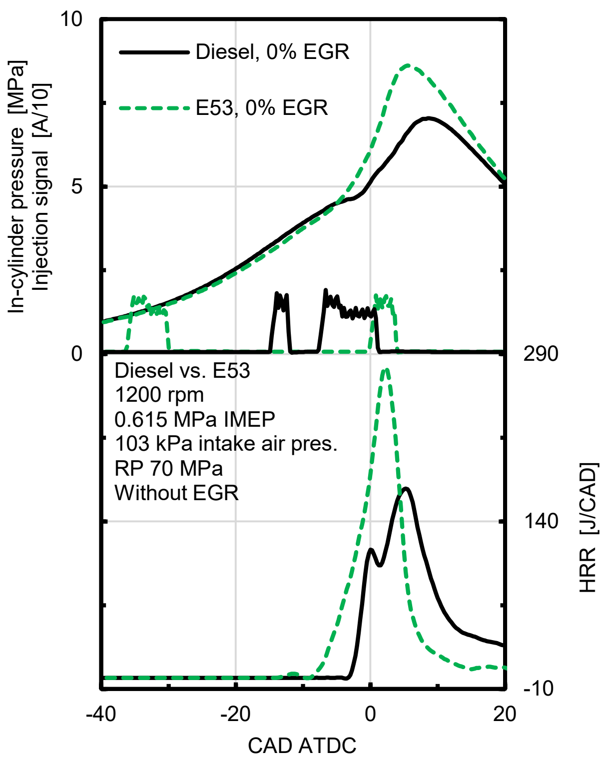

Figure 10 – In-cylinder pressure, injector signal, and HRR curves of the optimum ethanol-diesel combustion mode compared against a diesel case.

4.3 Effect of EGR on the optimum ethanol-diesel operating condition

Having identified an ethanol energy substitution ratio of 53% as the best trade-off in emissions and fuel consumption, further experiments were conducted to evaluate the effect of EGR in DF operation. The boundary conditions described in the previous sections were kept constant with the exception of intake manifold air temperature, which was elevated to 306±1 K due to the addition of 25% EGR at 343±5 K. As the control of combustion phasing in the DF mode relies on the diesel injection strategy, SOI_1 was fixed at ~-36.5 CAD ATDC with a constant energising timing ET_1 of 0.90 ms (i.e. 35 mm^3), providing a diesel injection split ratio of approximately 60/40. Experiments were carried out first with constant SOI_2 and then at constant CA50, by advancing SOI_2. Table 5 summarizes the diesel injection strategies, emissions, and performance of the two experiments with and without EGR.

In the case of constant SOI_2, adding EGR delayed combustion into the expansion stroke and increased the combustion duration. CA50 was retarded from 2.1 to 10.6 CAD ATDC and CA10-CA90 was extended from 13.5 to 17 CAD, drastically reducing NOx emissions from 3.56 to 0.69 g/kWh. Unlike the diesel-only operation, smoke emissions increased slightly from 0.011 to 0.018 g/kWh. Fuel consumption also increased with a more diluted charge and a longer second injection, necessary to keep the engine speed and IMEP constants. This caused a reduction in the ethanol energy fraction from 53 to 52%, as the amount of ethanol injected was held constant at 1.93 kg/h. CO and unburnt HC emissions also increased to a certain extent by the delayed and lower temperature combustion.

To keep constant CA50, the SOI_2 was advanced to phase the MFB profile closer to the CA50 of the 0% EGR case. However, as shown in Figure 11, introduction of EGR caused a longer ignition delay and consequently more time for the charge to mix. Once the combustion started, a more readily ignitable charge burnt in half the time. The higher global equivalence ratio and the longer mixing period resulted in a higher peak in-cylinder pressure and temperature, decreasing CO and unburnt HC emissions. NOx emissions were curbed by EGR. Net indicated efficiency with EGR was slightly lower than that without EGR, possibly as a consequence of non-optimized combustion phasing. As the Euro VI NOx and soot emissions targets have not been reached, further experiments were carried out by varying the first injection timing and diesel injection split ratio at a constant SOI_2, as described in the following section.

Table 5 – The effect of EGR on combustion, emissions, and efficiency of the optimum DF strategy running at an intake air pressure of 103 kPa and an RP of 70 MPa.

Parameter	Unit	E53, 0% EGR	E52, 25% EGR, same SOI_2	E53, 25% EGR, ~ same CA50
SOI_1	CAD ATDC	-36.1	-36.6	-36.6
ET_1	ms	0.90	0.90	0.90
ET_1	mm^3 (estimated)	35	35	35
SOI_2	CAD ATDC	0.2	0.2	-9.8
Split ratio	%	60/40	57/43	57/43
Ignition delay - SOI_2 to SOC	ms	-1.83	-0.75	0.29
COV_IMEP	%	1.4	1.5	1.1
Pmax	MPa	8.67	6.45	9.13
MPRR	MPa/CAD	0.94	0.56	1.82
CA50	CAD ATDC	2.1	10.6	1.9
CA10-CA90	CAD	13.5	17.0	6.9
$ISFC_{DF}$	g/kWh	184.4	189.9	186.2
Φ_{global}	-	0.44	0.63	0.60
ISSoot	g/kWh	0.011	0.018	0.013
ISNOx	g/kWh	3.56	0.69	2.73

ISCO	g/kWh	4.56	5.86	3.26
ISHC	g/kWh	4.90	5.41	3.62
Comb. eff.	%	97.4	97.1	98.1
Net ind. eff.	%	45.5	44.2	45.1

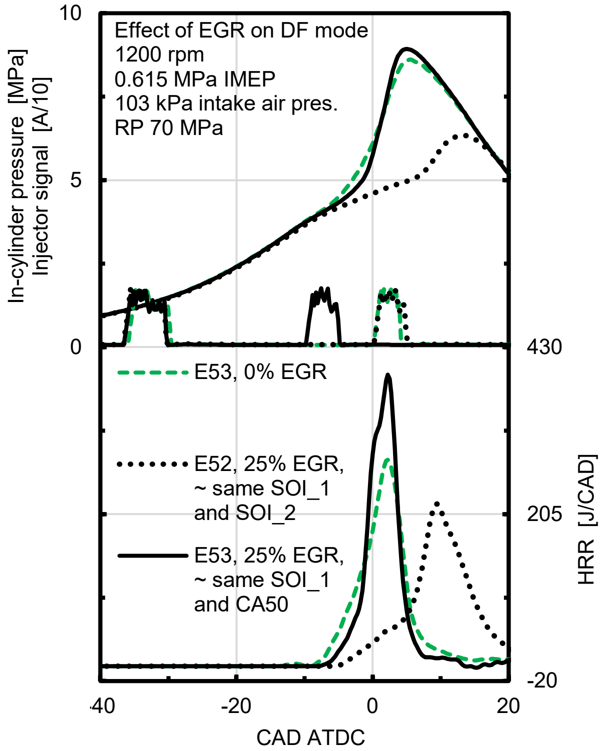

Figure 11 – In-cylinder pressure, injector signal, and HRR curves of the optimum DF strategy running with 0 and 25% EGR.

4.4 Effect of the first diesel injection timing and split ratio on the E53 operating condition

Sensitivity studies of the first diesel injection timing and the injection split ratio on combustion, emissions, and efficiency of the E53 mode were carried out in this section. This is prior to testing a higher diesel injection pressure and a lower equivalence ratio, which are addressed in the subsequent sections. The operating conditions for this series of experiments were the same as the previous section at an EGR rate of 25%. Unlike the prior tests with constant dwell timing, the SOI_2 was held at approximately -7.5 CAD

ATDC to provide a safety margin to MPRR and CA50. SOI_1 and ET_1 were varied at an injection pressure of 70 MPa.

An MPRR of 1.71 MPa/CAD was found with an SOI_1 occurring at -40 CAD ATDC at a diesel injection split ratio of approximately 57/43. It was also the calibration with the shortest combustion duration of 7.6 CAD, as depicted in Figure 12. Earlier injections reduced fuel-rich zones, which was supported by a drop in soot emissions and lowered charge reactivity. The result was a slower and retarded combustion process, increasing combustion losses and thus hindering the indicated efficiency. COV_IMEP also increased up to 1.7% in the most advanced SOI_1 case. However, later diesel pre-injections reduced the time available for mixing and regions of higher local equivalence ratio prevailed. This stratification advanced the CA50 and increased the maximum in-cylinder pressure and temperatures, resulting in higher NOx formation. Another consequence of over advanced combustion phasing was the increased compression work followed by the reduction in net indicated efficiency. Accordingly, the optimum emissions and efficiency trade-off was obtained by an SOI_1 event taking place around -36.5 CAD ATDC.

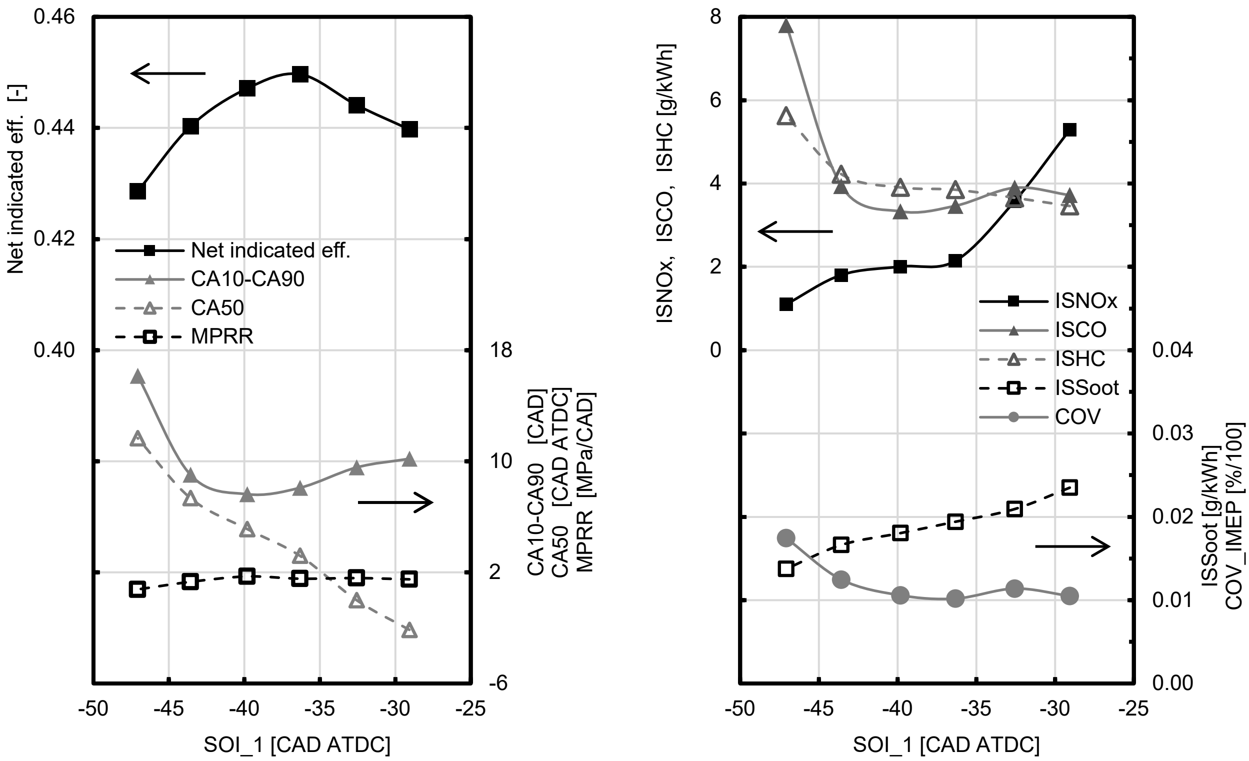

Figure 12 – Effect of the SOI_1 on combustion, emissions, and efficiency of the E53 mode running with a split ratio of ~57/43.

With an SOI_1 set at -36.5 CAD ATDC, the energising time of the first diesel injection was varied from 0.80 to 1.01 ms, representing 49 to 64% of the total energising time (i.e. 25 to 45 mm^3). The results obtained throughout this split ratio sweep are shown in Figure 13. Increasing the fuel quantity injected in SOI_1 yielded similar effects to retarding the first injection timing. At the largest first injection amount (i.e. split ratio of 64/36), the rapid and early combustion elevated the in-cylinder temperature and reduced unburnt HC and CO emissions at the expense of higher NOx and MPRR. Soot also increased as the mixing time available to the main injection was reduced, though the opposite was true for decreasing ET_1. The indicated efficiency fell for the smallest pre-injection amount (i.e. split ratio of 49/51) as a consequence of a less pre-mixed charge, which increased the burn rate and led to a later CA50. The optimum split ratio determined at this engine speed and load was an ET_1 equivalent to 53-55% of the total energising time (i.e. 30-35 mm^3). The COV_IMEP remained below 1.4%.

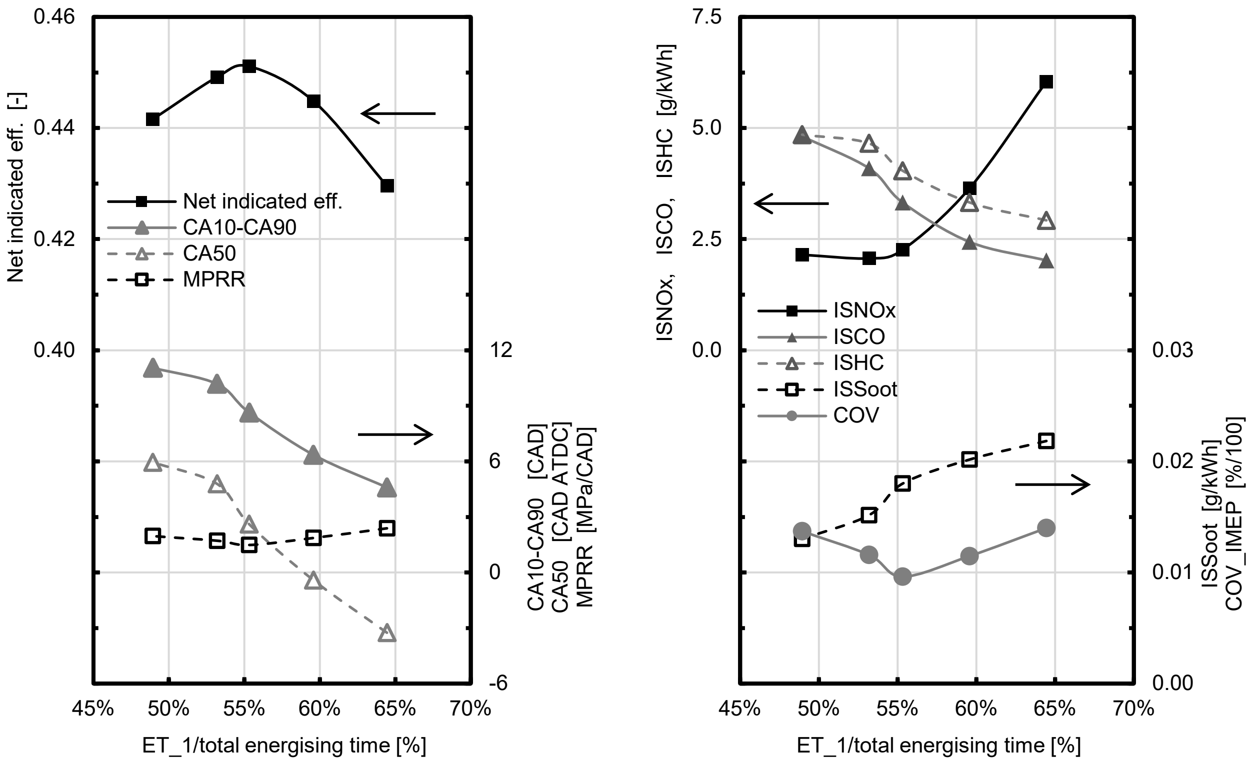

Figure 13 – Effect of split ratio on combustion, emissions and efficiency of the E53 mode running with an SOI_1 at -36.5 CAD ATDC.

4.5 Effect of higher intake air pressure and rail pressure on the E53 operating condition

With the goal to mitigate combustion losses and improve efficiency of ethanol-diesel combustion while reducing soot and NOx emissions to Euro VI legislation limits without the aid of aftertreatment systems, experiments with higher intake air pressure and diesel injection pressures were carried out for E53 with 25% EGR. For these experiments, the average ethanol substitution ratio was 53.4%, varying from 50.8 to 54.4% as the amounts of diesel fuel were automatically adjusted by the ECU to maintain a constant engine speed. Plots of two different rail pressures (70 and 90 MPa) and intake air pressures (103 and 125 kPa) were compared on a CA50 basis. The delta between the intake air pressure and the exhaust back pressure was held at 10 kPa. EGR was introduced into the system at 353±10 K, leading to intake air charge temperatures of 308±2 K. A pre-injection of ~30 mm^3, corresponding to diesel injection split ratio of approximately 54/46, was set at around -36.5 CAD ATDC. SOI_2 was altered accordingly within the range -9.5 to 1 CAD ATDC. Combustion stability was considered acceptable, with COV_IMEP between 0.9 and 2.2%.

Figure 14 depicts the in-cylinder pressure, injector signal, and MFB curves for a sweep of second injection timings at 125 kPa intake air pressure and 90 MPa injection pressure. As observed, despite of the fact that the SOC positions are similar, a retarded SOI_2 shifted the CA50 towards the expansion stroke, decreasing the peak in-cylinder pressure and increasing the CA10-CA90.

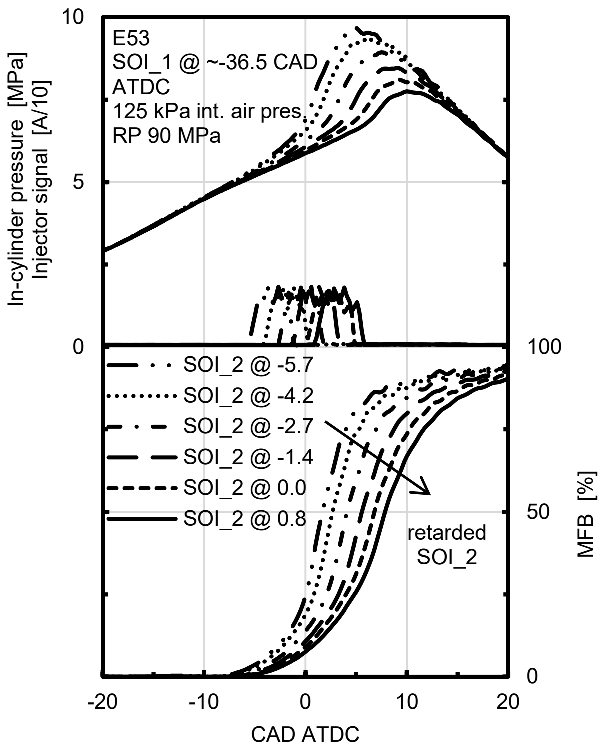

Figure 14 – In-cylinder pressure, injection signal, and MFB curves for a sweep of SOI_2.

To expand on this trend, SOI_2 and combustion duration with respect to CA50 for the two intake air pressures and two diesel injection pressures are shown in Figure 15. The diffusion combustion of the second diesel injection shifted CA50 into the expansion stroke and slowed down the burn rate of the premixed charge in all cases. A higher intake air pressure required a retarded SOI_2, possibly due to higher in-cylinder temperature that accelerated the SOC process of the mixture prior SOI_2. This is suggested by the low temperature heat release taking place even earlier in the most advanced cases. This fact is supported by the unexpected reduction in the ignition delay, highlighted by the circled region in Figure 16. Despite of the earlier SOC, the DF combustion at 125 kPa still possesses the longest CA10-CA90, which is a result of a lower global equivalence ratio and reduced charge reactivity.

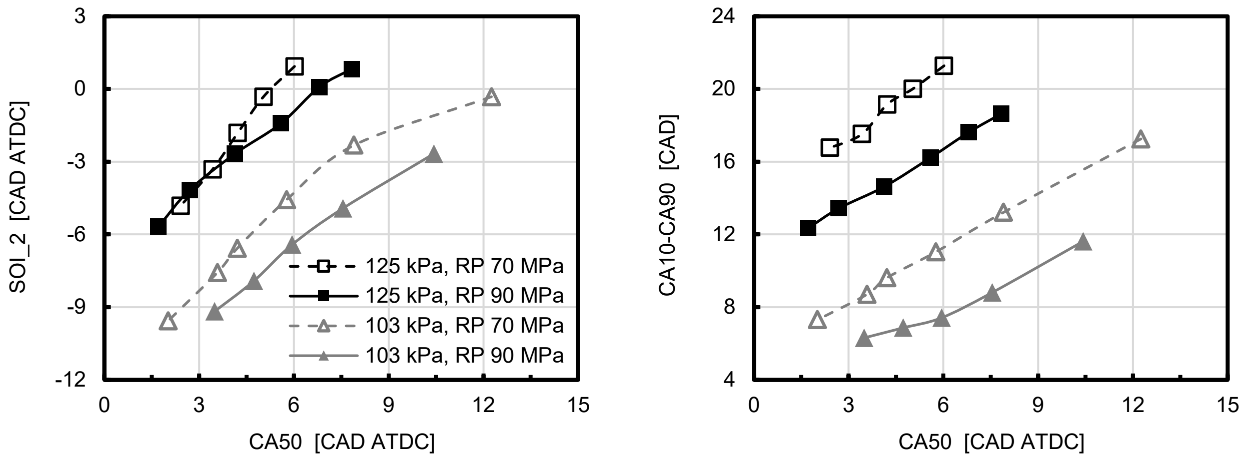

Figure 15 – SOI_2 and combustion duration vs. CA50.

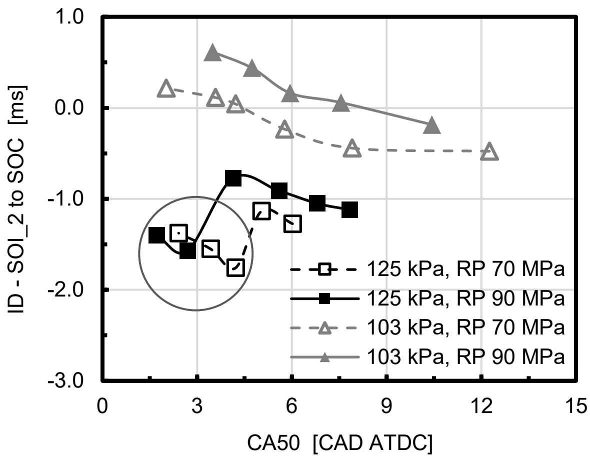

Figure 16 – Ignition delay from SOI_2 to SOC vs. CA50. Advanced SOI_2 at higher intake pressure, represented by the circled region, created in-cylinder conditions that initiate low temperature heat release.

Figure 17 presents the in-cylinder pressure, injector signal, and HRR curves of DF combustion running under different intake air and diesel injection pressures at a similar CA50 of ~5.8 CAD ATDC. A lower rail pressure required a retarded second diesel injection to obtain the same CA50. This occurs because a reduced RP creates ignition sites with a higher degree of stratification, advancing the start of combustion. An injection pressure of 90 MPa led to better atomization and a more homogeneous charge prior to the main injection, but higher PRR's (Figure 18) and shorter combustion durations. The MPRR was exceeded during the most advanced cases at 103 kPa intake air pressure. Another important observation concerns the HRR profile of the DF combustion mode running at a lower intake pressure and 90 MPa injection pressure. It is believed that the "double-hump" shape is a result of the fast burning of the second diesel injection followed by the ignition and combustion of the premixed charge, which creates the second HRR spike. As a result, elevated PRR and high NOx emissions were observed at this specific boost and diesel injection pressure.

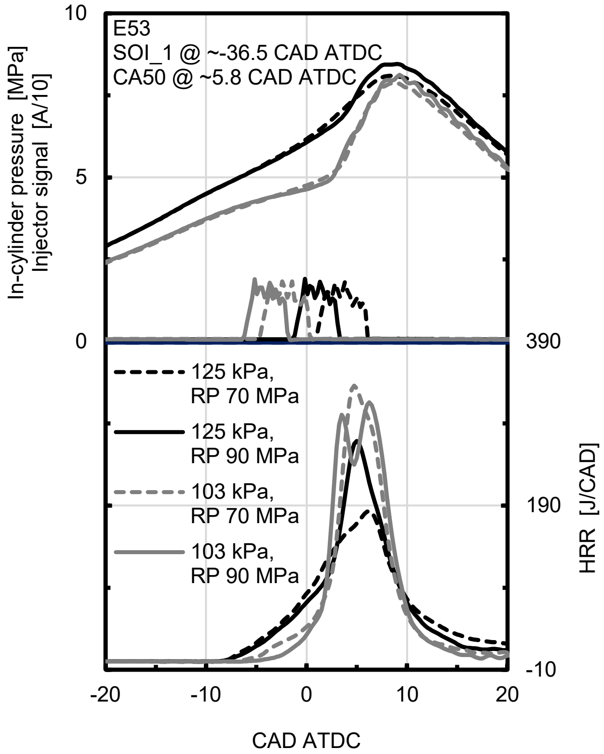

Figure 17 – Intake air and diesel injection pressures effect on in-cylinder pressure, injection timing, and HRR curves.

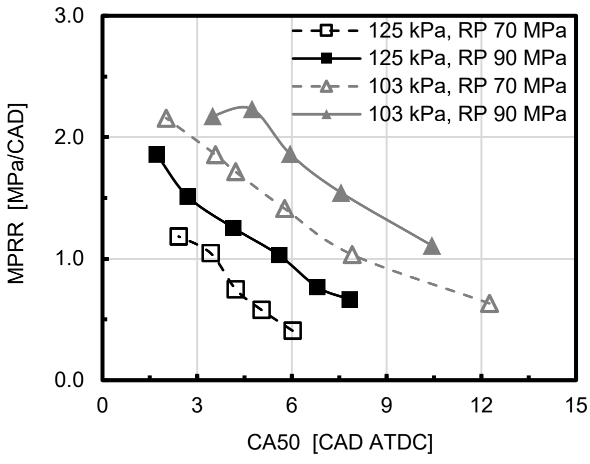

Figure 18 –MPRR vs. CA50.

Figure 19 shows the trade-offs of NOx and soot emissions, combustion efficiency, and net indicated efficiency. As stated previously, a retarded SOI_2 slowed down the combustion process and reduced in-cylinder peak pressure and temperature, resulting in decreased NOx emissions. Despite the higher in-cylinder pressure prior to the SOC at 125 kPa intake air pressure (see Figure 17), the lower global equivalence ratio decreased the reactivity of the premixed charge and heat release peaks, mitigating NOx formation. The opposite occurred when the rail pressure was increased, as a result of a faster combustion of the charge and the presence of close-to-stoichiometric regions. A higher injection pressure also improved mixture preparation, fuel efficiency, and smoke emissions. However, an advanced second injection at an intake air pressure of 103 kPa created relatively high temperature fuel-rich zones. The early second injection was poorly mixed and burnt too quickly (combustion duration of 6.3 CAD), leading to higher smoke readings. The operation at 125 kPa exhibited the opposite behaviour, with soot emissions increasing as SOI_2 was retarded. This is a consequence of low temperature fuel-rich regions and a delayed combustion process towards the expansion stroke.

Combustion efficiency in DF mode remains lower than diesel-only operation due to the reduced reactivity of the ethanol and the different combustion type. Ethanol flame propagation has flame quenching and forcing of unburnt charge into the combustion chamber crevices before the flame front arrival. Higher intake pressures and a retarded second injection increased combustion losses within the piston bowl and crevices up to 4%, mainly due to the lower local in-cylinder temperatures and over-lean regions. An intake air pressure of 103 kPa yielded contrary effects, leading to combustion efficiencies up to 98% due to higher global equivalence ratios, increasing in-cylinder temperatures and improving the flammability of the charge. The optimum DF operating points were then determined by the best $ISFC_{DF}$/ISNOx/ISSoot trade-off at an intake air pressure and a rail pressure of 125 kPa and 90 MPa, respectively. Two ethanol-diesel calibrations, shown in Table 6, were compared to the conventional diesel baseline trade-off:

(1) the operating point with optimum $ISFC_{DF}$/ISNOx/ISSoot trade-off in DF mode;

(2) the most fuel efficient operating point in DF mode.

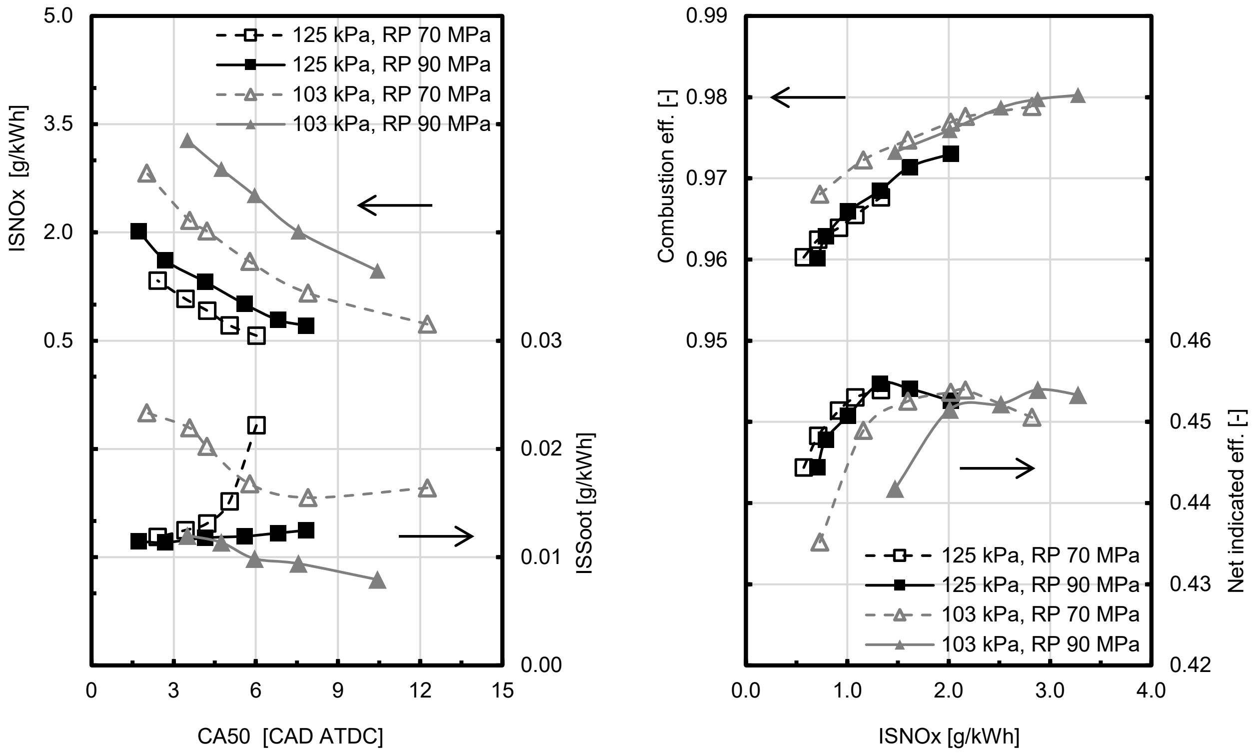

Figure 19 – The effect of different intake and injection pressures on emissions, combustion efficiency, and net indicated efficiency on the E53 operating condition.

Table 6 – Optimum diesel-only trade-off and DF calibrations, running with 25% EGR and 125 kPa intake air pressure.

Parameter	Unit	Diesel, trade-off	E53, trade-off	~E54, most fuel efficient
SOI_1	CAD ATDC	-9.3	-36.7	-36.7
ET_1	ms	0.38	0.76	0.76
ET_1	mm^3 (estimated)	3	30	30
SOI_2	CAD ATDC	-2.0	0.8	-2.7

Split ratio	%	30/70	53/47	55/45
Rail pressure	MPa	125	90	90
Ignition delay - SOI_2 to SOC	ms	0.49	-1.12	-0.77
COV_IMEP	%	1.8	1.6	1.4
Pmax	MPa	7.56	7.85	9.09
MPRR	MPa/CAD	1.42	0.67	1.26
CA50	CAD ATDC	9.2	7.8	4.1
CA10-CA90	CAD	22.3	18.6	14.6
$ISFC_{DF}$	g/kWh	190.4	188.8	184.5
EGT	K	596	578	567
Φ_{global}	-	0.53	0.51	0.50
ISSoot	g/kWh	0.0175	0.0125	0.0118
ISNOx	g/kWh	2.01	0.71	1.32
ISCO	g/kWh	0.67	9.55	6.94
ISHC	g/kWh	0.14	6.69	5.34
Comb. eff.	%	99.8	96.0	96.8
Net ind. eff.	%	44.1	44.4	45.5

It can be observed that a premixed charge of ethanol resulted in several benefits. These included higher indicated efficiency, and lower soot and NOx emissions than diesel-only operation. The use of optimized split diesel injections kept ISCO and ISHC below 10 g/kWh and demonstrated a considerable improvement in comparison to previous studies [39–42]. Exhaust gas temperature (EGT) presented lower values than conventional diesel combustion. Figure 20 compares the in-cylinder pressure, injector signal, and MFB curves of the optimum emissions trade-off in diesel-only and ethanol-diesel operating conditions against the most fuel efficient case attained during this study. Dual-fuel mode was characterized by advanced combustion phasing, shorter combustion durations and generally higher peak in-cylinder pressures. This can be attributed to the early diesel injection which increased the flammability of the in-cylinder charge and promoted a more reactive mixture prior to the second injection. The diesel injection close to TDC (SOI_2) determined the combustion phasing. It is believed that second injections might have less of an effect with higher ethanol substitution ratios due to auto-ignition of the premixed charge or misfire.

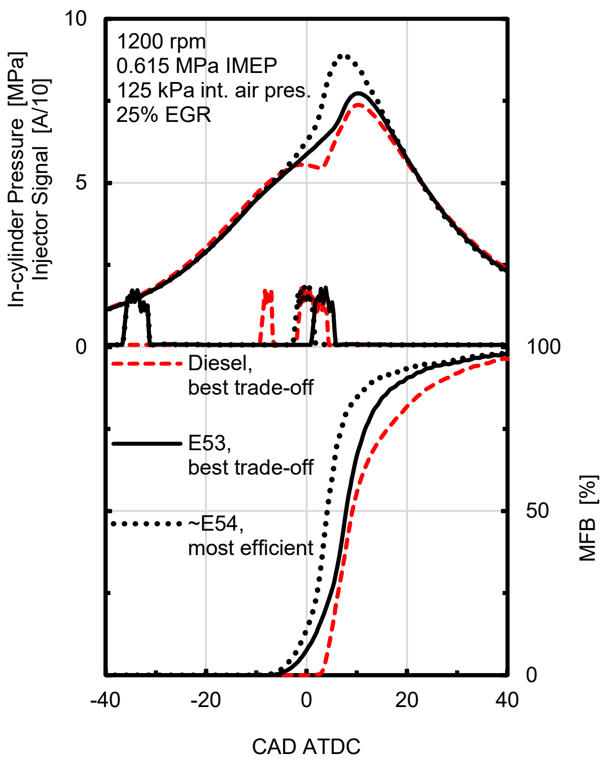

Figure 20 – In-cylinder pressure, injector signal, and MFB traces of the optimum emissions trade-off in diesel-only and DF modes compared against the most fuel efficient DF case.

Euro VI legislation emissions limits were not fully met under conventional diesel operation or dual-fuel mode. However, the best results were obtained with utilization of a renewable energy source. The advanced combustion concept of a premixed charge of ethanol ignited by diesel injections reduced NOx levels by 65% and soot emissions by approximately 33% when compared to diesel-only operation. As a result of its faster combustion and lower compression work, net indicated efficiency increased by nearly 3.2% in the most efficient DF case. The radar chart below (Figure 21) summarizes the main trends and behaviours of the optimum emissions trade-off and the most fuel efficient ethanol-diesel calibrations in comparison to the optimum conventional diesel combustion case. Net indicated efficiency, maximum in-cylinder pressure (Pmax), soot and NOx emissions, and combustion efficiency results were normalized to obtain a clear distinction of the benefits. The clear advantages of the DF mode are shown in terms of higher net indicated efficiency and substantially lower NOx and soot emissions, which are the main limiting factors of HD diesel engines. The majority of the unburnt HC and CO emissions produced by DF operation can be removed by an oxidation catalyst, assuming an EGT of approximately 570 K [55].

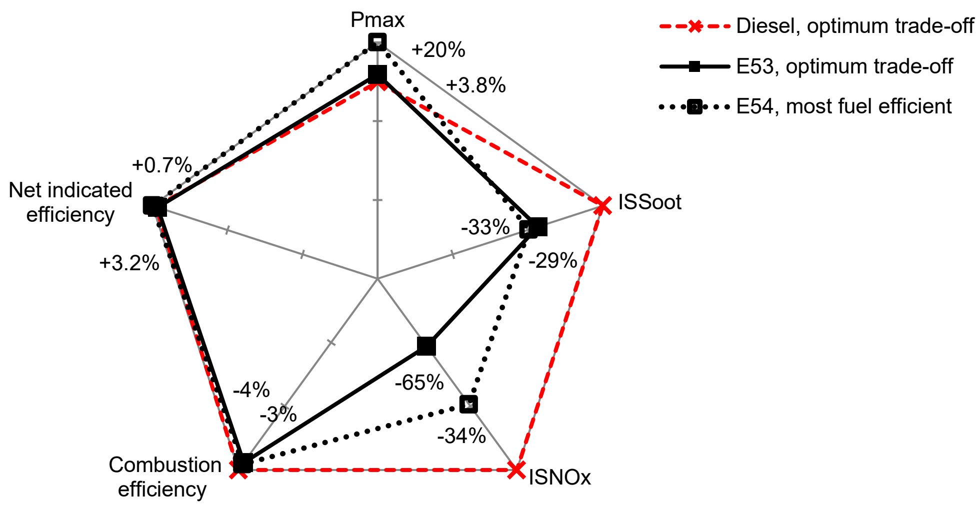

Figure 21 – Normalized net indicated efficiency, maximum in-cylinder pressure, ISSoot and ISNOx emissions, and combustion efficiency results of the optimum trade-offs in diesel and DF modes, and the most fuel efficient DF case.

5 Conclusions

In this paper, the optimization of ethanol-diesel combustion in a HD diesel engine operating at 25% load was experimentally investigated. The effects of three ethanol substitution ratios and several diesel injection strategies on combustion, emissions, and efficiency were analysed and discussed. Split diesel injections enabled an extended operating range and the best emissions and efficiency results in DF mode. Different split ratios and injection timings were studied at various intake and diesel injection pressures, with and without EGR. The main findings can be summarized as follows:

(1) Diesel-only combustion requires a combination of very high injection pressures and EGR rates to achieve low engine-out emissions of soot and NOx. Intake air pressure also needs to be increased to avoid a fuel economy penalty.

(2) Ethanol dual-fuel combustion with a single diesel injection close to TDC or a short pre-injection had no or limited operating range due to high MPRR and low indicated efficiency. A split diesel injection strategy allowed a better mixing preparation and created an in-cylinder charge reactivity distribution, increasing the fuel conversion efficiency.

(3) In the majority of the cases tested, the highly premixed charge in the DF mode lowered local in-cylinder temperatures and reduced fuel-rich zones, resulting in lower NOx and soot emissions than conventional diesel combustion. It also displayed faster combustion than diesel-only operation under a similar injection strategy. Additionally, the ethanol cooling effect reduced the compression work, allowing higher net indicated efficiencies.

(4) Higher ethanol substitution ratios, such as E68, resulted in lower fuel conversion efficiency at this particular load. This is due to incomplete combustion of ethanol caused by reduced charge temperature. Low substitution ratios, as E32, did not demonstrate large benefits in terms of emissions reduction and also resulted in lower net indicated efficiency.

(5) The optimum DF strategy without EGR was an ethanol substitution ratio of approximately 53%, with a diesel pre-injection timing between -40 and -35 CAD

ATDC, and a split ratio of ~60/40. The addition of EGR reduced NOx emissions and promoted longer ignition delays, consequently allowing more time for the charge to mix prior to the SOC.

(6) Earlier first injections reduced fuel-rich zones and lowered the charge reactivity. However, later first injections promoted higher local equivalence ratio zones of diesel, yielding opposite effects. Higher first injection amounts led to faster and earlier combustions with reduced unburned HC and CO emissions, but higher MPRR and NOx production. Soot also increased as the mixing time prior to SOC after the second injection was reduced. The opposite is true for a shorter first diesel injection.

(7) Unlike RCCI, the diesel injection strategy used in this work used a constant and early first injection combined to a later injection around TDC. This allowed control over the combustion phasing without varying fuel reactivity (i.e. ethanol substitution ratio). As the main injection was delayed, peak in-cylinder pressure also dropped and the burn rate increased.

(8) A reduced rail pressure in the DF mode created a higher degree of stratification, advancing the SOC and increasing soot emissions. However, it led to longer CA10-CA90 and lower NOx levels. A higher injection pressure delayed the SOC as a result of improved diesel atomization and a more homogeneous charge prior to the second injection. As a result, shorter combustion durations and increased MPRR and NOx emissions were experienced.

(9) A lower global equivalence ratio (higher intake pressure) decreased local reactivity zones in the premixed charge and heat release peaks, mitigating NOx formation. The drawback is an increase in combustion losses (i.e. unburnt HC and CO emissions).

In conclusion, dual-fuel combustion simultaneously achieved lower levels of NOx and soot in a HD diesel engine operating at low load with a moderate amount of EGR. Combustion losses were mitigated and a higher net indicated efficiency was also attained by using an optimized ethanol substitution ratio combined with split diesel injection strategies. Further work is being carried out to determine the optimum ethanol substitution fractions at different engine speeds and loads to obtain the highest possible utilization of biofuel while minimizing engine-out emissions.

Acknowledgment

The authors would like to acknowledge the Brazilian Ministry of Education and the Coordination for the Improvement of Higher Education Personnel (CAPES) for supporting the PhD studies of Mr. Pedrozo at Brunel University London.

References

[1] Reitz RD. Directions in internal combustion engine research. Combustion and Flame 2013;160:1–8. doi:10.1016/j.combustflame.2012.11.002.

[2] Imtenan S, Varman M, Masjuki HH, Kalam M a., Sajjad H, Arbab MI, et al. Impact of low temperature combustion attaining strategies on diesel engine emissions for diesel and biodiesels: A review. Energy Conversion and Management 2014;80. doi:10.1016/j.enconman.2014.01.020.

[3] Hikosaka N. A View of the Future of Automotive Diesel Engines. SAE Technical Paper 1997. doi:10.4271/972682.

[4] Zhao H. Advanced direct injection combustion engine technologies and development - Volume 2: Diesel engines. Cambridge: Woodhead Publishing Limited; 2010.

[5] U.S. Energy Information Adminstration. International Energy Outlook 2014. Washington: 2014.

[6] United Nations Environment Programme. Towards sustainable production and use of resources: assessing biofuels. 2009.

[7] Asad U, Zheng M, Ting DS-K, Tjong J. Implementation Challenges and Solutions for Homogeneous Charge Compression Ignition Combustion in Diesel Engines. Journal of Engineering for Gas Turbines and Power 2015;137. doi:10.1115/1.4030091.

[8] Bendu H, Murugan S. Homogeneous charge compression ignition (HCCI) combustion: Mixture preparation and control strategies in diesel engines. Renewable and Sustainable Energy Reviews 2014;38. doi:10.1016/j.rser.2014.07.019.

[9] Yao M, Zheng Z, Liu H. Progress and recent trends in homogeneous charge compression ignition (HCCI) engines. Progress in Energy and Combustion Science 2009;35:398–437. doi:10.1016/j.pecs.2009.05.001.

[10] Kook S, Bae C. Combustion Control Using Two-Stage Diesel Fuel Injection in a Single-Cylinder PCCI Engine. SAE Technical Paper 2004. doi:10.4271/2004-01-0938.

[11] Neely GD, Sasaki S, Huang Y, Leet J a, Stewart DW. New Diesel Emission Control Strategy to Meet US Tier 2 Emissions Regulations. SAE Technical Paper 2005. doi:10.4271/2005-01-1091.

[12] Kook S, Bae C, Miles PC, Choi D, Pickett LM. The Influence of Charge Dilution and Injection Timing on Low-Temperature Diesel Combustion and Emissions. SAE Technical Paper 2005. doi:10.4271/2005-01-3837.

[13] Opat R, Ra Y, Gonzalez D. MA, Krieger R, Reitz RD, Foster DE, et al. Investigation of Mixing and Temperature Effects on HC/CO Emissions for Highly Dilute Low Temperature Combustion in a Light Duty Diesel Engine. SAE Technical Paper 2007. doi:10.4271/2007-01-0193.

[14] Musculus MPB, Miles PC, Pickett LM. Conceptual models for partially premixed low-temperature diesel combustion. Progress in Energy and Combustion Science 2013;39. doi:10.1016/j.pecs.2012.09.001.

[15] Kimura S, Aoki O, Ogawa H, Muranaka S, Enomoto Y. New Combustion Concept for Ultra-Clean and High-Efficiency Small DI Diesel Engines. SAE Technical Paper 1999. doi:10.4271/1999-01-3681.

[16] Hasegawa R, Yanagihara H. HCCI Combustion in DI Diesel Engine. SAE Technical Paper 2003. doi:10.4271/2003-01-0745.

[17] Sellnau M, Foster M, Hoyer K, Moore W, Sinnamon J, Husted H. Development of a Gasoline Direct Injection Compression Ignition (GDCI) Engine. SAE International Journal of Engines 2014;7:835–51. doi:10.4271/2014-01-1300.

[18] Sellnau M, Moore W, Sinnamon J, Hoyer K, Foster M, Husted H. GDCI Multi-Cylinder Engine for High Fuel Efficiency and Low Emissions. SAE International Journal of Engines 2015;8. doi:10.4271/2015-01-0834.

[19] Kalghatgi GT, Risberg P, Ångström H-E. Partially Pre-Mixed Auto-Ignition of Gasoline to Attain Low Smoke and Low NOx at High Load in a Compression Ignition Engine and Comparison with a Diesel Fuel. SAE Technical Paper 2007. doi:10.4271/2007-01-0006.

[20] Manente V, Zander C, Johansson B, Tunestal P, Cannella W. An Advanced Internal Combustion Engine Concept for Low Emissions and High Efficiency from Idle to Max Load Using Gasoline Partially Premixed Combustion. SAE Technical Paper 2010. doi:10.4271/2010-01-2198.

[21] Manente V, Johansson B, Cannella W. Gasoline partially premixed combustion, the future of internal combustion engines? International Journal of Engine Research 2011;12:194–208. doi:10.1177/1468087411402441.

[22] Manente V, Johansson B, Tunestal P. Characterization of Partially Premixed Combustion With Ethanol: EGR Sweeps, Low and Maximum Loads. Journal of Engineering for Gas Turbines and Power 2010;132. doi:10.1115/1.4000291.

[23] Shen M, Tuner M, Johansson B, Cannella W. Effects of EGR and Intake Pressure on PPC of Conventional Diesel, Gasoline and Ethanol in a Heavy Duty Diesel Engine. SAE Technical Paper 2013;01. doi:10.4271/2013-01-2702.

[24] Shen M, Tuner M, Johansson B. Close to Stoichiometric Partially Premixed Combustion - The Benefit of Ethanol in Comparison to Conventional Fuels. SAE Technical Paper 2013. doi:10.4271/2013-01-0277.

[25] Kaiadi M, Johansson B, Lundgren M, Gaynor J a. Experimental Investigation on different Injection Strategies for Ethanol Partially Premixed Combustion. SAE Technical Paper 2013. doi:10.4271/2013-01-0281.

[26] Eichmeier J, Wagner U, Spicher U. Controlling Gasoline Low Temperature Combustion by Diesel Micro Pilot Injection. Journal of Engineering for Gas Turbines and Power 2012;134. doi:10.1115/1.4005997.

[27] Reitz RD, Duraisamy G. Review of high efficiency and clean reactivity controlled compression ignition (RCCI) combustion in internal combustion engines. Progress in Energy and Combustion Science 2015;46:12–71. doi:10.1016/j.pecs.2014.05.003.

[28] Benajes J, Molina S, García A, Belarte E, Vanvolsem M. An investigation on RCCI combustion in a heavy duty diesel engine using in-cylinder blending of diesel and gasoline fuels. Applied Thermal Engineering 2014;63:66–76. doi:10.1016/j.applthermaleng.2013.10.052.

[29] Kokjohn SL, Hanson RM, Splitter DA, Reitz RD. Experiments and Modeling of Dual-Fuel HCCI and PCCI Combustion Using In-Cylinder Fuel Blending. SAE International Journal of Engines 2009;2. doi:10.4271/2009-01-2647.

[30] Kokjohn SL, Hanson RM, Splitter D a., Reitz RD. Fuel reactivity controlled compression ignition (RCCI): a pathway to controlled high-efficiency clean combustion. International Journal of Engine Research 2011;12:209–26. doi:10.1177/1468087411401548.

[31] Padala S, Woo C, Kook S, Hawkes ER. Ethanol utilisation in a diesel engine using dual-fuelling technology. Fuel 2013;109:597–607. doi:10.1016/j.fuel.2013.03.049.

[32] Sarjovaara T, Alantie J, Larmi M. Ethanol dual-fuel combustion concept on heavy duty engine. Energy 2013;63:76–85. doi:10.1016/j.energy.2013.10.053.

[33] He B, Wang J, Shuai S, Yan X. Homogeneous Charge Combustion and Emissions of Ethanol Ignited by Pilot Diesel on Diesel Engines. SAE Technical Paper 2004. doi:10.4271/2004-01-0094.

[34] Han X, Xie K, Tjong J, Zheng M. Empirical Study of Simultaneously Low NOx and Soot Combustion With Diesel and Ethanol Fuels in Diesel Engine. Journal of Engineering for Gas Turbines and Power 2012;134. doi:10.1115/1.4007163.

[35] Gao T, Divekar P, Asad U, Han X, Reader GT, Wang M, et al. An Enabling Study of Low Temperature Combustion With Ethanol in a Diesel Engine. Journal of Energy Resources Technology 2013;135:042203. doi:10.1115/1.4024027.

[36] Divekar P, Yang Z, Ting D, Chen X, Zheng M, Tjong J. Efficiency and Emission Trade-Off in Diesel-Ethanol Low Temperature Combustion Cycles. SAE Technical Paper 2015. doi:10.4271/2015-01-0845.

[37] Han X, Zheng M, Tjong J. Clean combustion enabling with ethanol on a dual-fuel compression ignition engine. International Journal of Engine Research 2015:1–13. doi:10.1177/1468087415575646.

[38] Han X, Divekar P, Reader G, Zheng M, Tjong J. Active Injection Control for Enabling Clean Combustion in Ethanol-Diesel Dual-Fuel Mode. SAE International Journal of Engines 2015;8:890–902. doi:10.4271/2015-01-0858.

[39] Júnior RFB, Martins CA. Emissions analysis of a diesel engine operating in Diesel-Ethanol Dual-Fuel mode. Fuel 2014;148:191–201. doi:10.1016/j.fuel.2014.05.010.

[40] Fang W, Huang B, Kittelson DB, Northrop WF. Dual-Fuel Diesel Engine Combustion with Hydrogen, Gasoline and Ethanol as Fumigants: Effect of Diesel Injection Timing. Journal of Engineering for Gas Turbines and Power 2014;136. doi:10.1115/1.4026655.

[41] Ogawa H, Shibata G, Kato T, Zhao P. Dual Fuel Diesel Combustion with Premixed Ethanol as the Main Fuel. SAE Technical Paper 2014. doi:10.4271/2014-01-2687.

[42] Asad U, Kumar R, Zheng M, Tjong J. Ethanol-fueled low temperature combustion: A pathway to clean and efficient diesel engine cycles. Applied Energy 2015. doi:10.1016/j.apenergy.2015.01.057.

[43] Heywood JB. Internal Combustion Engine Fundamentals. vol. 21. 1st ed. McGraw-Hill, Inc.; 1988.

[44] Silvis WM. An Algorithm for Calculating the Air/Fuel Ratio from Exhaust Emissions. SAE Technical Paper 1997. doi:10.4271/970514.

[45] Zhao H, Ladammatos N. Engine Combustion Instrumentation and Diagnostics. Warrendale, Pa. USA: 2001.

[46] Kar K, Cheng WK. Speciated Engine-Out Organic Gas Emissions from a PFI-SI Engine Operating on Ethanol/Gasoline Mixtures. SAE International Journal of Fuels and Lubricants 2009;2:91–101. doi:10.4271/2009-01-2673.

[47] Wallner T. Correlation Between Speciated Hydrocarbon Emissions and Flame Ionization Detector Response for Gasoline/Alcohol Blends. Journal of Engineering for Gas Turbines and Power 2011;133. doi:10.1115/1.4002893.

[48] AVL. AVL 415SE Smoke Meter - Product Guide. Graz, Austria: 2013.

[49] Economic Commission for Europe of the United Nations (UN/ECE). Regulation No 49. 2013.

[50] Splitter DA, Reitz RD. Fuel reactivity effects on the efficiency and operational window of dual-fuel compression ignition engines. Fuel 2014;118. doi:10.1016/j.fuel.2013.10.045.

[51] Kokjohn SL, Hanson R, Splitter D, Kaddatz J, Reitz R. Fuel Reactivity Controlled Compression Ignition (RCCI) Combustion in Light- and Heavy-Duty Engines. SAE International Journal of Fuels and Lubricants 2011;4. doi:10.4271/2011-01-0357.

[52] Fang W, Kittelson DB, Northrop WF. An Experimental Investigation of Reactivity-Controlled Compression Ignition Combustion in a Single-Cylinder Diesel Engine Using Hydrous Ethanol. Journal of Energy Resources Technology 2015;137. doi:10.1115/1.4028771.

[53] Dempsey AB, Das Adhikary B, Viswanathan S, Reitz RD. Reactivity Controlled Compression Ignition Using Premixed Hydrated Ethanol and Direct Injection Diesel. Journal of Engineering for Gas Turbines and Power 2012;134. doi:10.1115/1.4006703.

[54] Tutak W. Bioethanol E85 as a fuel for dual fuel diesel engine. Energy Conversion and Management 2014;86:39–48. doi:10.1016/j.enconman.2014.05.016.

[55] Tsang KS, Zhang ZH, Cheung CS, Chan TL. Reducing Emissions of a Diesel Engine Using Fumigation Ethanol and a Diesel Oxidation Catalyst. Energy & Fuels 2010;24. doi:10.1021/ef100899z.

Glossary

ATDC	After Firing Top Dead Centre
CA10-CA90	Combustion Duration (10-90% Cumulative Heat Release)
CA50	Crank Angle of 50% Cumulative Heat Release
CAD	Crank Angle Degree
CO	Carbon Monoxide
CO_2	Carbon Dioxide
COV_IMEP	Coefficient of Variation of the IMEP
DAQ	Data Acquisition
DF	Dual-Fuel
DT	Dwell Timing
ECR	Effective Compression Ratio
ECU	Engine Control Unit
EGR	Exhaust Gas Recirculation
EGT	Exhaust Gas Temperature
ESC13	European Stationary Cycle
ET	Energising Time
ET_1	First Injection Energising Time
ET_2	Second Injection Energising Time
FID	Flame Ionization Detector
FSN	Filter Smoke Number
GDCI	Gasoline Direct Injection Compression Ignition
GHG	Greenhouse Gas
HC	Hydrocarbons
HCCI	Homogeneous Charge Compression Ignition
HD	Heavy-Duty
HPP	High-Pressure Diesel Pump

HRR	Apparent Net Heat Release Rate
iEGR	Internal Exhaust Gas Recirculation
IMEP	Net Indicated Mean Effective Pressure
ISFC	Net Indicated Specific Fuel Consumption
ISCO	Net Indicated Specific Emissions of CO
ISHC	Net Indicated Specific Emissions of Unburnt HC
ISNOx	Net Indicated Specific Emissions of NOx
ISSoot	Net Indicated Specific Emissions of Soot
IVC	Intake Valve Closing
LTC	Low Temperature Combustion
MFB	Mass Fraction Burned
MK	Modulated Kinetics
NOx	Mono-Nitrogen Oxides
O_2	Oxygen
Pmax	Maximum In-cylinder Pressure
PCCI	Premixed Charge Compression Ignition
PFI	Port Fuel Injector
PM	Particulate Matter
PMPC	Premixed Micro Pilot Combustion
PPC	Partially Premixed Combustion
PPCI	Partially Premixed Charge Compression Ignition
RCCI	Reactivity Controlled Compression Ignition
RP	Rail Pressure
SOC	Start of Combustion
SOI	Start of Injection
SOI_1	First Injection Timing

SOI_2	Second Injection Timing
TDC	Firing Top Dead Centre
UNIBUS	Uniform Bulky Combustion System
VVA	Variable Valve Actuation
WHSC	World Harmonized Stationary Cycle
γ	Ratio of Specific Heats
Φ_{global}	Global Equivalence Ratio

Appendix – Measurement Device Specifications

Measured Variable	Device	Manufacturer	Dynamic Range	Linearity/ Accuracy	Repeatability
CO (low content)	AIA-721A	Horiba (MEXA 7170 DEGR)	0-2.5k ppm	≤ ± 1.0% FS or ± 2.0% of readings	Within ± 0.5% of FS
CO (mid-high content)	AIA-722		0-12 vol%		
CO_2	AIA-722		0-20 vol%		
NOx	CLA-720MA		0-500 ppm or 0-10k ppm		
O_2	MPA-720		0-25 vol%		
Unburnt HC	FIA-725A		0-500 ppm or 0-50k ppm		
Diesel injector current signal	Current Probe PR30	LEM	0-20 A	± 1% of reading ± 2 mA	
Diesel flow rate (return)	PROline promass 83A DN01	Endress+ Hauser	0-100 kg/h	± 0.10% of reading	± 0.05% of reading
Diesel flow rate (supply)	PROline promass 83A DN02		0-20 kg/h	± 0.10% of reading	± 0.05% of reading
Intake and exhaust pressures	Piezoresistive pressure sensor Type 4049A Amplifier Type 4622A	Kistler	0-1 MPa	≤ ± 0.50% of FS within 0-353 K	
In-cylinder pressure	Piezoelectric pressure sensor Type 6125C	Kistler	0-30 MPa	≤ ± 0.40% of FS	
	Amplifier FI Piezo	AVL		≤ ± 0.01% of FS	
Intake valve lift	S-DVRT-24 Displacement Sensor DEMOD-DVRT-TC conditioner	LORD MicroStrain	0-24 mm	± 1% of reading using straight line	± 1.0 µm
Intake air mass flow rate	Proline t-mass 65F	Endress+ Hauser	0-910 kg/h	± 1.5% of reading (10 to 100% of FS)	±0.5% of reading
Oil and ethanol pressure	Pressure transducer UNIK 5000	GE	0-1 MPa	< ±0.20% of FS	
Smoke Number	415SE	AVL	0-10 FSN	-	Within ± 0.005 FSN + 3% of reading
Speed	AG150 Dynamometer	Froude Hofmann	0-8000 rpm	± 1 rpm	
Torque			0-500 Nm	± 0.25% of FS	
Temperature	Thermocouple K Type (Class 2)	RS	233-1473 K	≤ ± 2.5 K or ± 0.75% of readings	

* FS = full scale